Fish and Shellfish Immunology 110 (2021) 1–9

Contents lists available at ScienceDirect

Fish and Shellfish Immunology

journal homepage: www.elsevier.com/locate/fsi

Full length article

Comparative study of coelomocytes from *Arbacia lixula* and *Lythechinus variegatus*: Cell characterization and *in vivo* evidence of the physiological function of vibratile cells

Vinicius Queiroz [a,*], Sandra M. Muxel [a], Luigi Inguglia [b], Marco Chiaramonte [b], Márcio R. Custódio [a]

[a] Department of Physiology, Institute of Biosciences, University of São Paulo, São Paulo, Brazil
[b] Dept. STEBICEF, University of the Study of Palermo, Via Archirafi 18, 90123, Palermo, Italy

ARTICLE INFO

Keywords:
Cytology
Echinoderm immunity
Imaging flow cytometry
Invertebrate physiology
Phagocytes
Red spherulocyte

ABSTRACT

The knowledge on echinoderm coelomocytes has increased in recent years, but researchers still face a complex problem: how to obtain purified cells. Even flow cytometry being useful to address coelomocytes in suspension, the need for a method able to provide isolated cells is still noteworthy. Here, we use Imaging Flow Cytometry (IFC) to characterize the coelomocytes of two sea urchin species – *Arbacia lixula* and *Lytechinus variegatus* – and obtain gates to isolate cell populations. Then, we used these gates to study the physiological response of *A. lixula* coelomocytes during an induced immune challenge with *Escherichia coli*. An analysis of area and aspect ratio parameters of the flow cytometer allowed the identification of two main cell populations in the coelomic fluid: circular and elongated cells. A combination of this method with nucleus labeling using propidium iodide allowed the determination of gates containing isolated subpopulations of vibratile cells, red spherulocytes, and two phagocytes subpopulations in both species. We observed that during an induced bacterial immune challenge, *A. lixula* was able to modulate coelomocyte frequencies, increasing the phagocytes and decreasing red spherulocytes and vibratile cells. These results indicate that vibratile cells and red spherulocytes act by immobilizing and stoping bacterial growth, respectively, cooperating with phagocytes in the immune response. The use of IFC was fundamental not only to identify specific gates for the main coelomic subpopulations but also allowed the investigation on how echinoids modulate their physiological responses during immune challenges. Furthermore, we provide the first experimental evidence about the role of vibratile cells, corroborating its involvement with the immune system.

1. Introduction

Echinoderms are marine deuterostome invertebrates characterized by their calcareous endoskeleton and remarkable pentamerous symmetry [1]. They typically have six to eight main cell types in their coelomic fluid [2]. These cells, termed coelomocytes, are important for physiological functions such as regeneration [3], phagocytosis [4], encapsulation of foreign matter [5], and clotting [6]. Recent studies examined these cells at different levels, including morphology and ultrastructure [7], physiological functions [8,9], biotechnological applications [10], and their potential use for bio-monitoring [11].

Regardless of the research topic, two main approaches have been commonly employed in studies addressing echinoderm coelomocytes: the use of samples containing all coelomic cell types or of semi-purified populations [10]. For the latter, the most common method is based on standard protocols of centrifugation in density gradients using sucrose [12], Percoll [13], or Ficoll [14], among others [8]. However, these methods yield only enriched fractions, containing more than one cell type [8].

For flow cytometry, although numerous attempts to discriminate echinoderm coelomocytes have been made [15,16], the low number of fluorescent markers for specific cell types of echinoderms [17,18] has limited the results. Consequently, most works using flow cytometry have relied only on structural parameters, *i.e.* side and forward scatter [19,20], but in these studies, gates for specific cell populations have scarcely been defined, and again only enriched subpopulations are obtained [16,

* Corresponding author. Rua do Matão, n° 321, Cidade Universitária, São Paulo, SP, CEP: 05508-090, Brazil.
E-mail address: vinicius_ufba@yahoo.com.br (V. Queiroz).

https://doi.org/10.1016/j.fsi.2020.12.014
Received 15 September 2020; Received in revised form 19 December 2020; Accepted 22 December 2020
Available online 27 December 2020

20].

The main problem when working with flow cytometry is similar to that seen when using gradient methods: specific coelomocytes can undergo a sequence of maturation stages [2,7]. During this process, density, size, and/or granularity of different populations overlap with that of other cell types. This restricts the separation of monotypic layers, in the case of density gradients, or the identification of gates containing isolated populations in cytometers [20].

The ability to study isolated cell types is important not only for know the diversity in echinoderm coelomocytes, but also to understand the physiology of each subpopulation, which ultimately may be used as a tool for monitoring organisms' health status. In general, it is known that the coelomocyte percentage is altered during physiological stresses such as microorganism infection [21] or wound healing [3]. However, specific responses need to be clarified yet. In echinoids, for example, the baseline of phagocytes and red spherulocytes, cells involved in phagocytosis and bactericidal activity respectively [22], is significantly altered during exposition to lypopolysaccharides (LPS) [9] or bacterial cells [21]. However, evidence on the dynamics and physiological contribution of another cell type during stressful conditions are scarce. In this sense, any new method capable of analyzing specific subpopulations will provide not only a tool for monitoring health status but will also make it possible to understand the physiological role of poorly studied coelomocytes.

In recent years, imaging flow cytometry (IFC) has been adopted in several studies on vertebrates (*e.g.* human cells and/or extracellular corpuscles [23]), and its use to investigate invertebrate cells has begun [24,25]. This method produces digital images of every single registered particle, which can then be analyzed in combination with the typical cytometry parameters to obtain additional data from the cell suspension. As stated by Barteneva et al. [26] 'this method allows for the acquisition and identification of tens of thousands of cellular events based on their fluorescent and morphological parameters'. Under this method, the traditional identification of coelomocytes based on their morphology [7] can be considerably useful to analyze the different cell types, as well as improve studies in echinoderm physiology.

Thus, we aimed to investigate here, through a comparative approach, how imaging flow cytometry could be useful to obtain isolated populations (gates). Posteriorly, we used one of the species to analyze how these gates may be useful as a tool to access the physiological status of the echinoderms. To achieve these goals, we used the coelomic cells of two sea urchin species: *Arbacia lixula* and *Lytechinus variegatus*. The reasoning for choosing these echinoids was based on two main points: (1) they are common species in the southeastern Brazilian coast, easy to collect and maintain in confinement, and they have been studied under different perspectives [27,28]; (2) there is a considerable amount of physiological and immunological information about both species [29–31]. The DNA/nucleus dye propidium iodide and a correlation between area and aspect ratio parameter were used to produce gates containing specific subpopulations of both species. The IFC was applied to investigate the *in vivo* cellular responses of coelomocytes of *A. lixula* in an experimental bacterial immune challenge with *Escherichia coli*. In addition to the response of phagocytes and red spherulocytes, we observed changes in the vibratile cells, corroborating its involvement in sea urchin immune response. Lastly, we propose a model to explain how phagocytes, red spherulocytes, and vibratile cells interact to maintain sea urchin homeostasis. Our results indicate that IFC can be used for characterizing coelomocytes and for investigating changes in the response of each cell type to physiological alterations.

2. Material and methods

2.1. Study animals and immune cell collection

Two sea urchin species, the camarodont *Lytechinus variegatus* (LV) and the arbacioid *Arbacia lixula* (AL) were collected from the São

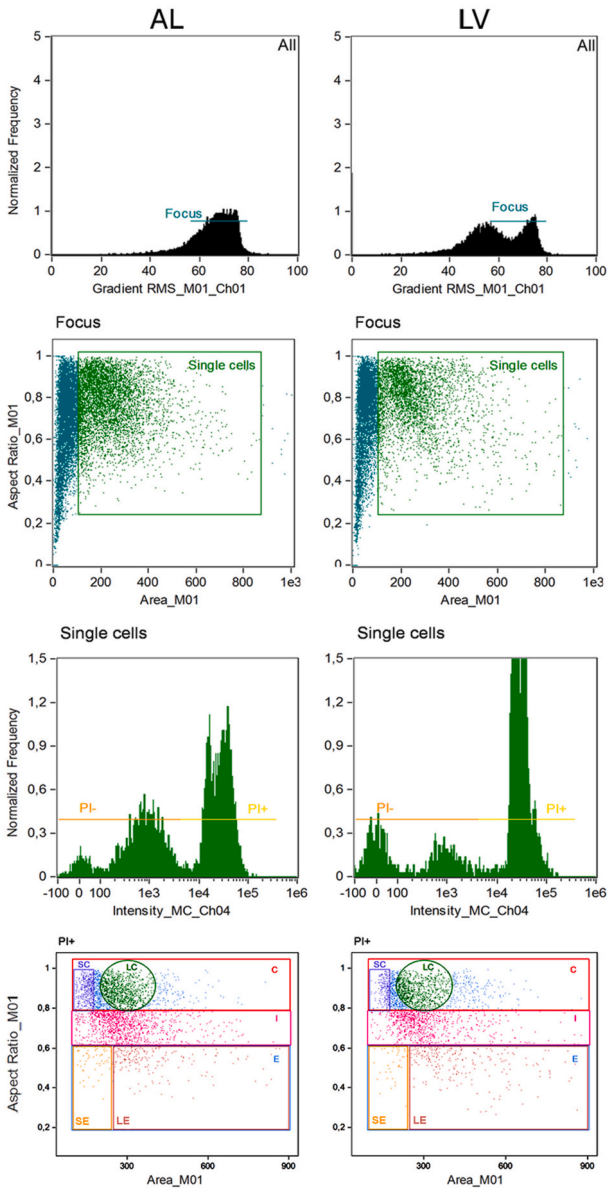

Fig. 1. Histogram of focused cells (row 1) gated based on RMS gradients of brightfield channels for *Arbacia lixula* (AL) and *Lytechinus variegatus* (LV). The single-cell population (row 2) was determined in the focused cells (row 3) and was based on aspect ratio versus area parameters of the brightfield channel. The histogram of PI-labeled (PI^+) cells was based on the intensity of channel 4 and adjusted to gate subpopulations (row 4). Three main gates were assigned as indicated by circular (C), subdivided in small circular (SC) and large circular (LC); intermediate (I); and elongated (E), subdivided in small elongated (SE) and large elongated (LE).

Sebastião Channel, São Paulo State, Brazil, and transferred to the Instituto de Biociências – Universidade de São Paulo. The coelomic fluid of three individuals of each species was collected by inserting a needle into the peristomial membrane and aspirating the fluid into a syringe containing 1.5 mL of a fixation medium (2.5% glutaraldehyde) in an isosmotic anticoagulant solution (20 mM ethylenediaminetetraacetic acid (EDTA), 460 mM sodium chloride, 7 mM sodium sulfate, 10 mM potassium chloride, 10 mM 4-(2-hydroxyethyl)-1-piperazineethanesulfonic acid, at pH 8.2 – [32]). Equal volumes of coelomic fluid were collected, and the samples were stored at 4 °C for at least 6 h. After fixation, cell suspensions were centrifuged at 150 × g for 10 min using an Eppendorf 5804R centrifuge, and the supernatant was removed. The cells were then resuspended using the anticoagulant

solution, and the procedure repeated three times to remove the fixation medium. Cell density was then counted using a Neubauer chamber, adjusted to 1×10^7 cells/mL using the anticoagulant solution, and 50 μL was used for cytometric analyses. Additional samples were collected from other specimens (n = 9) as described above; however, immediately before cytometric analyses, cells were labeled using 1 μg/mL propidium iodide (PI). In this analysis, only PI-positive particles were considered. To reduce differences regarding physiological competencies and coelomic fluid volumes, 21 similar-sized specimens of AL (4–5 cm in test diameter) were used for the infection experiments. All animals used were kept at room temperature in seawater tanks for one week to allow acclimation before the experiments, as described in Queiroz [33].

2.2. Imaging flow cytometer data acquisition and analysis

Data acquisition was performed at the Central de Aquisição de Imagens e Microscopia of the Instituto de Biociências (CAIMI-IB) using an imaging flow cytometer (FlowSight, Amnis-Merck Millipore). Acquisition speed was set to 'low', and the highest resolution was used. Roughly 20,000 cells were acquired based on their *area* (as pixels) and *aspect ratio*, defined as the value of the minor axis divided by the major cell axis on channel 1. The focused cells were gated using root mean squared (RMS) gradient, based on channel 1. Channels 1, 4, and 6 were used to analyze brightfield, PI labeling, and side scatter (SSC) parameters, respectively, using IDEAS software (Amnis-Merck Millipore). Cell debris and doublets were gated out based on area and aspect ratio features as indicated in Fig. 1. Singlet cells were gated to separate PI-positive cells based on channel 4, and subpopulations of coelomocytes were determined based on area vs. aspect ratio (Fig. 1). The width parameter was based on channel 1. Data on the width and cell percentage are presented as means ± standard error of the mean. Differences in percentage means between treatments (PI^+ and no PI) or species were tested using a Student's two-tailed *t*-test at $p < 0.05$.

2.3. Bacterial culture and immune challenge procedures

Escherichia coli (strain ATTC 11229) were cultured for 24 h before the experiments using LB nutrient broth [34] at 37 °C. The culture was collected after centrifugation at 5000 × g for 15 min. The supernatant was removed, and *E. coli* were mixed with sterile-filtered (pore size 0.22 μm) natural seawater at a concentration of 1×10^9 cells/mL [35]. Specimens of AL were injected through the peristome with 1 mL of *E. coli* (treatment group) or with the same volume of sterile natural seawater (control group) using a hypodermic needle. This volume was injected in two different places in the perivisceral coelom, to avoid an excessive introduction of bacteria in a single spot. Before this experiment, the averages cell density and coelomic fluid volume in the coelom of AL were determined as $8.7 \times 10^6 \pm 1.5 \times 10^6$ cells/mL and 6–7 mL per individual (n = 5). Thus, considering 6.5 mL as the mean coelomic fluid volume per individual, and the mean cell density found here, we injected 1 mL of *E. coli* (1×10^9 cells/mL) in the perivisceral cavity, which resulted in a final proportion of 15–21 bacteria per coelomocyte in the treatment group. The number of the injected bacterial cell in the echinoids was adapted from Canesi et al. [36].

2.4. Experimental design

Twenty-one specimens of AL were assigned to one of two groups: the treatment group, which was injected with *E. coli* in sterile natural seawater (n = 9), and the control group, which was injected with sterile-filtered natural seawater (n = 9). Non injected animals (n = 3), named t_0, were sampled just before the start of the experiment and used as a parameter to untreated organisms. All individuals of the control and treatment groups were injected at the beginning of the experiment (t_0), and at 24, 48, and 72 h the coelomic cells of three individuals were collected at the same time of the day (10:00 h). Cells were fixated and analyzed as described above. Only PI-positive cells were considered in this analysis. Cell percentages were compared using a two-way analysis of variance (ANOVA), with time post-infection and treatment as factors, followed by Tukey multiple comparison tests when applicable. Differences were considered significant if $p < 0.05$.

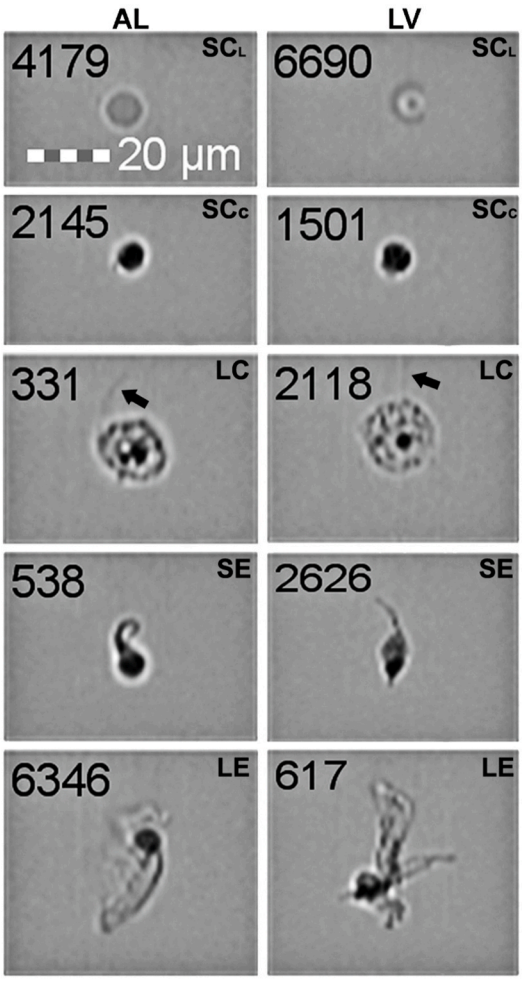

Fig. 2. Coelomocytes of *Arbacia lixula* (AL) and *Lytechinus variegatus* (LV) without propidium iodide labeling. Subpopulations of coelomocytes were based on aspect ratio, area, and granularity (SSC). Legend: small circular less (SC_L), small circular complex (SC_C), large circular (LC), small elongated (SE), and large elongated (LE), flagellum (arrow). The number on each image indicates the frame registered by the device.

3. Results

3.1. Identifying coelomocyte populations on IFC

Using only the aspect ratio vs. area features, the coelomocytes were assigned to two major populations: circular cells ([C]; aspect ratio 0.78–1, area 100–900) and elongated cells ([E]; aspect ratio 0.2–0.6, area 100–900; Fig. 1). Within these two broad categories, most coelomocyte subpopulations present in the coelomic fluid, *i.e.* phagocytes, vibratile cells, and spherulocytes, were identified in gates containing isolated cells using IFC. In the circular population, two different groups were observed: the first comprised small circular cells ([SC]; aspect ratio 0.78–1, area 100–200), and the second group comprised large circular cells ([LC]; aspect ratio 0.78–1, area 250–450). In the elongated population, only phagocytes were observed, which were subdivided into small elongated cells ([SE]; aspect ratio 0.2–0.6, area 100–300) and large elongated cells ([LE]; aspect ratio 0.2–0.6, area 300–900; Fig. 1).

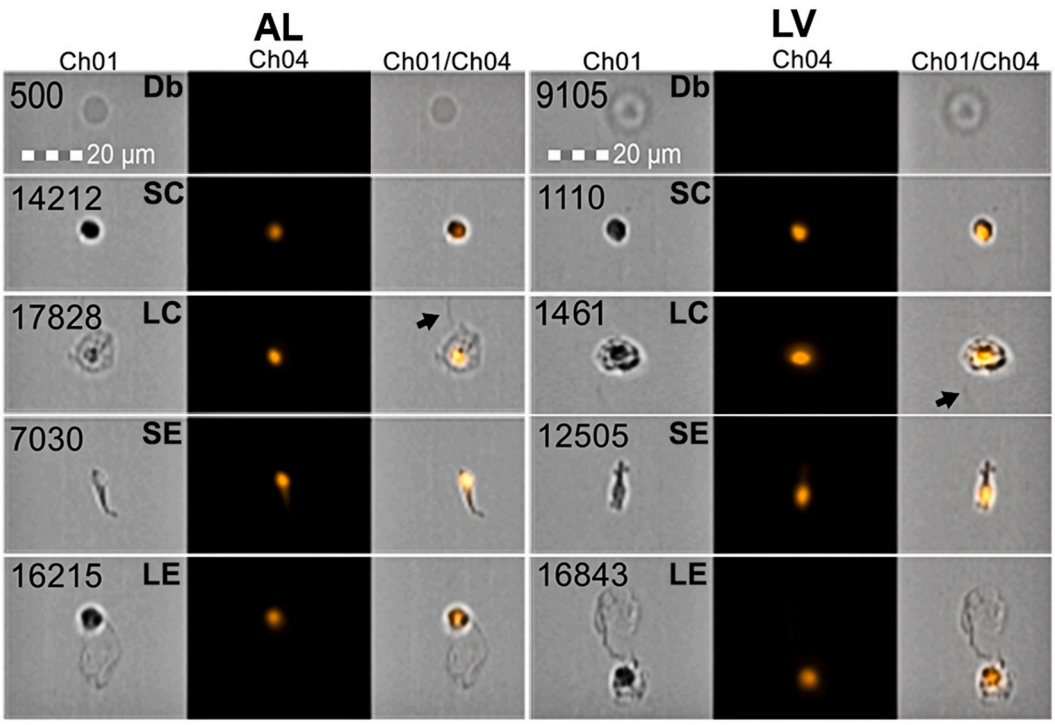

Fig. 3. Propidium iodide labeled (PI^+) coelomocytes of *Arbacia lixula* (AL) and *Lytechinus variegatus* (LV). From left to right: brightfield (channel 1 - gray), PI^+ fluorescence (channel 4 - orange), and merging of the fluorescence and brightfield channels. Legend: debris (Db), small circular (SC), large circular (LC), small elongated (SE), large elongated (LE), flagellum (black arrow). The number on each image indicates the frame registered by the device.

Table 1
Percentage and width of coelomocytes measured by imaging flow cytometry in different sea urchin species with and without propidium iodide.

Species	Parameter	Treatment	C	SC	LC	E	SE	LE	I
AL	**Percentage (%)**	**PI^+**	57.17 ± 1.83A*	11.77 ± 1.22A*	29.39 ± 0.79A*	9.33 ± 1.13A*	1.74 ± 0.07A*	7.05 ± 1.09A*	33.08 ± 0.88A
		No PI	40.78 ± 0.15a	23.73 ± 2.66a	10.86 ± 1.81a	23.76 ± 0.75a	20.30 ± 1.36a	3.46 ± 0.64a	33.25 ± 1.22a
	Width (μm)	**PI^+**	16.61 ± 0.06	13.15 ± 0.03	17.73 ± 0.03	16.99 ± 0.14	12.89 ± 0.54	18.14 ± 0.08	16.96 ± 0.23
		No PI	14.31 ± 0.25	12.14 ± 0.03	19.5 ± 0.02	13.85 ± 0.19	11.98 ± 0.02	19.5 ± 0.02	15.74 ± 0.05
LV	**Percentage (%)**	**PI^+**	59.44 ± 1.83A*	8.09 ± 1.58B*	29.22 ± 0.85A*	9.74 ± 0.65A*	1.54 ± 0.15A*	7.94 ± 0.63A*	30.41 ± 1.53A*
		No PI	41.25 ± 1.44a	12.12 ± 0.01b	18.04 ± 0.06b	29.05 ± 0.99b	19.67 ± 2.20a	9.38 ± 1.43b	27.38 ± 0.86b
	Width (μm)	**PI^+**	16.96 ± 0.25	13.34 ± 0.01	17.62 ± 0.17	16.93 ± 0.29	12.75 ± 0.11	18.55 ± 0.24	17.55 ± 0.19
		No PI	16.27 ± 0.38	11.58 ± 0.03	18.76 ± 0.16	15.08 ± 0.29	11.77 ± 0.06	20.41 ± 0.22	16.09 ± 0.25

AL = *Arbacia lixula*; LV = *Lytechinus variegatus*; PI^+ = Propidium iodide labeled cells; No PI = Unlabeled cells; C = Circular; I = Intermediate; E = Elongated; SC = Small circular; LC = Large circular; SE = Small elongated; LE = Large elongated. * = Asterisk indicates significant differences ($p < 0.05$) between treatments in the same species (PI x No PI). Different letters indicate significant differences ($p < 0.05$) between species (upper case = PI^+; lower case = No PI).

Cell populations in the intermediate region ([I]; aspect ratio 0.6–0.8, area 100–900) were heterogeneous as a mix of all subpopulations described above was observed in this gate.

3.2. Characteristics of coelomocytes based on IFC

Regardless of the species analyzed, morphology and width were considerably specific to each cell population, which facilitated coelomocyte recognition (Figs. 2 and 3; Table 1). Nevertheless, PI labeling was necessary to verify cell identification, mainly inside the SC gate. In the initial analyses, this area contained objects with contrasting morphologies in which the usual parameters (aspect ratio × area) could not be used for population separation. According to their granularity and opacity based on SSC characteristics, SC were divided into two subgroups: 'less complex' SC (SC_L) and 'complex' SC (SC_C; Fig. 2). To ensure that particles identified as SC_L were not in fact debris, the cells were labeled with PI, and further analyses were conducted. Labeled nuclei were only observed in SC_C, indicating that SC_L particles were debris (Fig. 3). Regarding other cell types, both unlabeled and PI-labeled cells provided similar results; however, to avoid potential errors, all descriptions were based exclusively on PI-labeled samples.

The SC were characterized as dark and visibly vacuolated coelomocytes (Figs. 2 and 3), while the LC subpopulation comprised large round cells with a central nucleus, granulous cytoplasm, and typically with a visible flagellum (*i.e.* vibratile cells – Figs. 2 and 3). The SE comprised phagocytes with a peripheral nucleus and short cytoplasmic expansions (Figs. 2 and 3). The LE were phagocytes with remarkable cytoplasmic expansions and with a subcentral nucleus, which was almost two-fold larger than that in SE (Figs. 2 and 3; Table 1). For each coelomic subpopulation, widths were very similar in both species (Table 1).

3.3. Coelomocyte frequency in different sea urchin species

The distribution of the main coelomic populations in gates C, I, and E, was very similar in both species, considering PI-labeled samples. However, there were some differences in the frequency of non-labeled coelomocytes (Table 1). Gate C comprised most cells (57.17 ± 1.83% in AL, and 59.44 ± 1.83% in LV) followed by I, which varied from 33.08 ± 0.88% in AL to 30.41 ± 1.53 in LV, and the less abundant elongated cells (E), ranging from 9.33 ± 1.13% in AL to 9.74 ± 0.65 in LV

Table 2
Summary table of two-way ANOVA applied to the cell percentages of *Arbacia lixula* experimentally infected with *Escherichia coli*.

Source of Variance	F	df	p
Gate C			
Time	18.25	(3, 16)	<0.0001
Treatment	15.06	(1, 16)	0.0013
Interaction	2.474	(3, 16)	0.0989 ^{NS}
Gate LC			
Time	18.42	(3, 16)	<0.0001
Treatment	8.05	(1, 16)	0.0119
Interaction	2.899	(3, 16)	0.0673 ^{NS}
Gate SC			
Time	9.569	(3, 16)	0.0007
Treatment	6.481	(1, 16)	0.0216
Interaction	5.346	(3, 16)	0.0096
Gate E			
Time	20.45	(3, 16)	<0.0001
Treatment	15.59	(1, 16)	0.0012
Interaction	5.001	(3, 16)	0.0123
Gate LE			
Time	22.92	(3, 16)	<0.0001
Treatment	4.566	(1, 16)	0.0484
Interaction	8.871	(3, 16)	0.0011
Gate SE			
Time	1.442	(3, 16)	0.2675 ^{NS}
Treatment	0.269	(1, 16)	0.6111 ^{NS}
Interaction	0.5114	(3, 16)	0.6802 ^{NS}
Gate I			
Time	12.16	(3, 16)	0.0002
Treatment	6.575	(1, 16)	0.0208
Interaction	7.084	(3, 16)	0.0030

NS = not significant ($p > 0.05$).

(Table 1). The frequency of specific coelomocyte subpopulations in unlabeled samples differed from that in PI-labeled ones (Table 1). In *A. lixula*, SC cells were the most abundant coelomocyte type in unlabeled samples, followed by SE and LC, while in the species *L. variegatus*, SE, LC, and SC were respectively the most abundant cell types. LE cells were the most uncommon cell type in both species (Table 1). In contrast, in PI-labeled samples, LC were by far the most abundant coelomocytes (29.39 ± 0.79% in AL and 29.22 ± 0.85% in LV), followed by SC (11.77 ± 1.22% in AL and 8.09 ± 1.58% in LV; Table 1). LE were the third-most abundant cell type (7.05 ± 1.09% in AL, and 7.94 ± 0.63% in LV), and SE were the least abundant coelomocyte type (1.74% in AL, and 1.54% in LV). Except for SC, there were no significant differences between species (Table 1).

3.4. Experimental immune challenge

Differences in *A. lixula* coelomocyte frequencies (and numbers) of general and specific cell types (Supplementary Material 1) were affected by the time, treatment, as well as the interaction of these two factors (Table 2), and could be observed mainly 48 and 72 h after *E. coli* injection (Fig. 4). In general, while cell frequency in the gate C was lower in the treatment than in the control group (except for SC before 72 h), the frequencies in the gate E (apart from SE) and I were higher in treatment than in control (Fig. 4). The frequency of cells in the t_0 (untreated animals) was generally similar to the control group (24, 48, and 72 h) in the gates C, E, and I, but differed significantly from treated individuals (Fig. 4).

The two-way ANOVA showed that the cells frequency in the gate C was affected by time ($F = 18.25$; $P < 0.0001$) and treatment ($F = 15.06$; $P = 0.0013$), but there was no significant interaction ($F = 2.474$; $P = 0.0989$). The treatment decreased the frequency of circular cells over the course of the experiment (to about 15% after 24, 48, and 72 h) compared to the untreated group (Fig. 4A). Control group was consistently different from treatment, mainly after 48 and 72 h (Fig. 4A). The same general pattern was observed in LC, which was affected by time ($F = 18.42$; $P < 0.0001$), treatment ($F = 8.05$; $P = 0.0119$), but not by the interaction of these factors ($F = 2.899$; $P = 0.0673$). In this gate, the percentage of cells decreased by nearly 20% in the treatment group, compared to control group (at 48 h; Fig. 4B). In contrast, SC was affected by both factors (time ($F = 9.569$; $P = 0.0007$); treatment ($F = 6.481$; $P = 0.0216$)), and by their interaction ($F = 5.346$; $P = 0.0096$). The treatment led to an increase in SC abundance of almost 50% after 24 h, but to a reduction after 48 and 72 h, compared to the control (Fig. 4C).

Elongated cells, which were affected by time ($F = 20.45$; $P < 0.0001$), treatment ($F = 15.59$; $P = 0.0012$), and their interaction ($F = 5.001$; $P = 0.0123$), were remarkably less abundant than circular cells (Fig. 4A and D), as well as showed a distinct pattern in response to *E. coli* injections with higher abundance in the treatment than in the control group. The time ($F = 5.001$; $P = 0.0123$), treatment ($F = 5.001$; $P = 0.0123$) and their interaction ($F = 5.001$; $P = 0.0123$) affected LE frequencies, but none of them affected SE percentages (Time ($F = 1.442$; $P = 0.2675$); Treatment ($F = 0.269$; $P = 0.6111$); Interaction ($F = 0.5114$; $P = 0.6802$)). The treatment promoted an increase in the abundance of elongated cells after 72 h (about 55%; Fig. 4D), of large elongated (LE) phagocytes after 48 h (about 40%; Fig. 4E), and smaller elongated cells after 72 h (about 80%; Fig. 4F). Cell frequency in gate I, which was affected by time ($F = 12.16$; $P = 0.0002$), treatment ($F = 6.575$; $P = 0.0208$), and their interaction ($F = 7.084$; $P = 0.0030$). Frequencies in this gate increased in the treatment group after 48 h (about 15%), whith a subsequent decrease after 72 h, compared to the control (Fig. 4G), which match with the dynamics of elongated cells.

4. Discussion

4.1. Coelomocyte populations

Using imaging flow cytometry (IFC), we achieved three important goals: (1) gates for isolated coelomic populations (Fig. 1 and Supplementary Material 2), (2) evidence that IFC is a suitable method to access echinoderm physiology, and (3) the first experimental data of vibratile cell activity.

Most of the coelomocyte subpopulations described in sea urchins were identified in the present study. The gate containing LC clearly comprised vibratile cells, which are the only flagellated coelomocytes in echinoids, while SC cells were composed of red spherulocytes. These were rather granular and showed darker coloration in the brightfield due to echinochrome-A. No cells morphologically similar to colorless spherulocytes were discriminated against. Although four main types of coelomocytes are typically recognized in echinoids, *i.e.* phagocytes, vibratile cells, and red and colorless spherulocytes [2,22], few studies using flow cytometry have succeeded in discriminate coelomocytes other than phagocytes (vibratile cells [37]; red spherulocytes [38,39]). By contrast, even not providing gates with isolated populations, a work using IFC identified six coelomic populations in the sea star *Marthasterias glacialis* [25]. Thus, our data certainly indicates that IFC can be quite useful to characterize echinoderm coelomocytes.

Two distinct phagocyte subpopulations were observed in both echinoid species using IFC. While LE (large phagocytes) correspond to the petaloid form of discoidal and polygonal phagocytes, due to its bladder-like expansions, SE cells matched the small phagocytes described by Gross et al. [40]. Studies on live sea urchin phagocytes in suspension have reported petaloid and filopodial forms [2]. Nevertheless, small phagocytes and discoidal and polygonal cells are typically observed only after the cells attach and spread out on a flat surface [40,41]. Cells morphologically similar to LE and SE observed using IFC were found in the sea star *Dermasterias imbricate* using scanning electron microscopy [42], and LE cells found here were also observed in the sea star *M. glacialis* using IFC [25]. As far as we know, only Coteur et al. [43] successfully differentiated phagocytic subpopulations in echinoderms through conventional flow cytometry.

The gate C and I showed a higher frequency in comparison to gate E, which contained phagocytes. Previous studies referred to phagocytes as

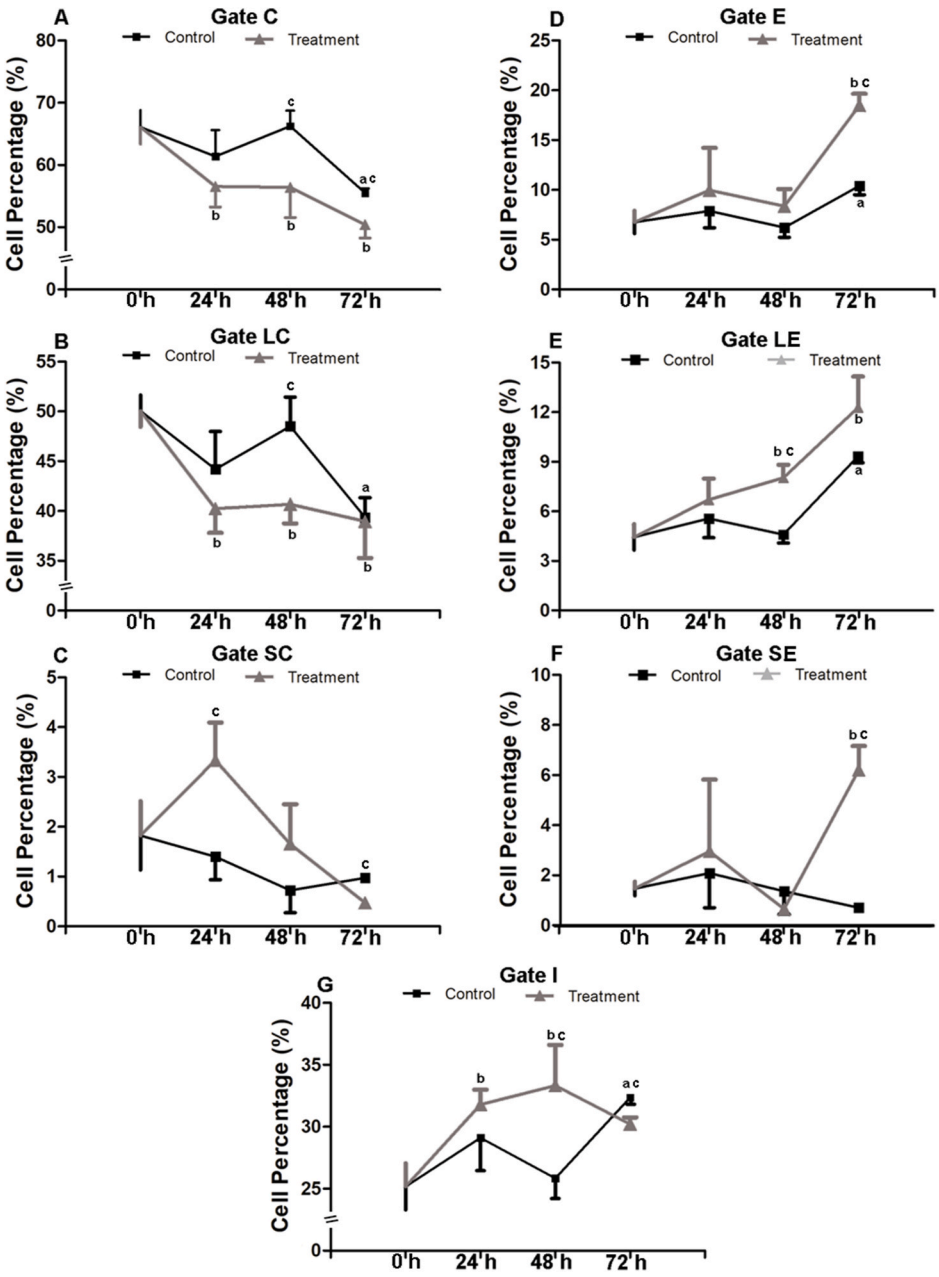

Fig. 4. Coelomic cell dynamics of *Arbacia lixula* injected with *Escherichia coli*. A – Circular cells; B – Large circular cells; C – Small circular cells; D – Elongated cells; E – Large elongated cells; F – Small elongated cells; G – Intermediate cells. Legend: C = circular cells; LC = large circular; SC = small circular; E = Elongated; LE = large elongated; SE = small elongated; I = intermediate; letters indicate statistical significance (Tukey multiple comparison test after a two way Anova; $p < 0.05$): a = comparison of different time points in control group to untreated animals (0 h); b = comparison of different time points in treatment group to untreated animals (0 h); c = comparison of treatment versus control group at the same time. Vertical lines in the graphs (upward and/or downward) indicate the standard deviation of each mean.

the most frequent coelomocyte in Echinoidea [4,44,45], however, this observation was not confirmed by our results. Numerous phagocytes were observed in the intermediate region. As highlighted in the echinoderm literature [11], petaloid and filopodial cell morphology probably corresponds to different stages of the same cell type. Thus, considering that only fixed cells were analyzed, the fast fixation method used here may have captured phagocytes in a transitional state and made them appear more rounded than elongated, which may have led to an underestimation of the actual proportion of this subpopulation.

LC and LE cells were more frequent in the PI-labeled treatment, while SC and SE were more common in the unlabeled one. The frequency of small coelomocytes (*i.e.* SC and SE) in the unlabeled treatment ranged from 1.5 to 12-fold higher than in the PI-labeled treatment The detection of small debris as whole cells, as preliminary observed with the SC_L population in the initial analysis, explain such difference in cell frequency. In this context, our results reinforce the importance to use PI-labeling or other nuclear markers to distinguish coelomocytes.

4.2. Experimental immune challenge

In the present study, we also stimulated the immune system of AL by injecting live *E. coli* – a bacteria commonly used in assays with marine invertebrate [46,47] – in the perivisceral coelom of this echinoid and observed coelomocyte population dynamics over 72 h. Studies assessing immune challenges in echinoderms over more than 24 h are scarce [42,48], and most involved the assessment of the first few hours after infection, typically only up to 48 h [48].

Opposed trends in cell frequencies were observed in infected animals: the number of circular cells (gate C) decreased, whereas elongated coelomocytes (gate E) increased, compared to the control. In the holothuroid *Holothuria glaberrima,* individuals stimulated with different pathogen-associated molecular patterns (PAMPs) also showed an increase in the number of phagocytes and a decrease in the number of type-1 spherulocytes [49]. Similar dynamics were found in the initial response of the echinoids *Paracentrotus lividus, Strongylocentrotus droebachiensis,* and *S. purpuratus*. In the first, although only the initial

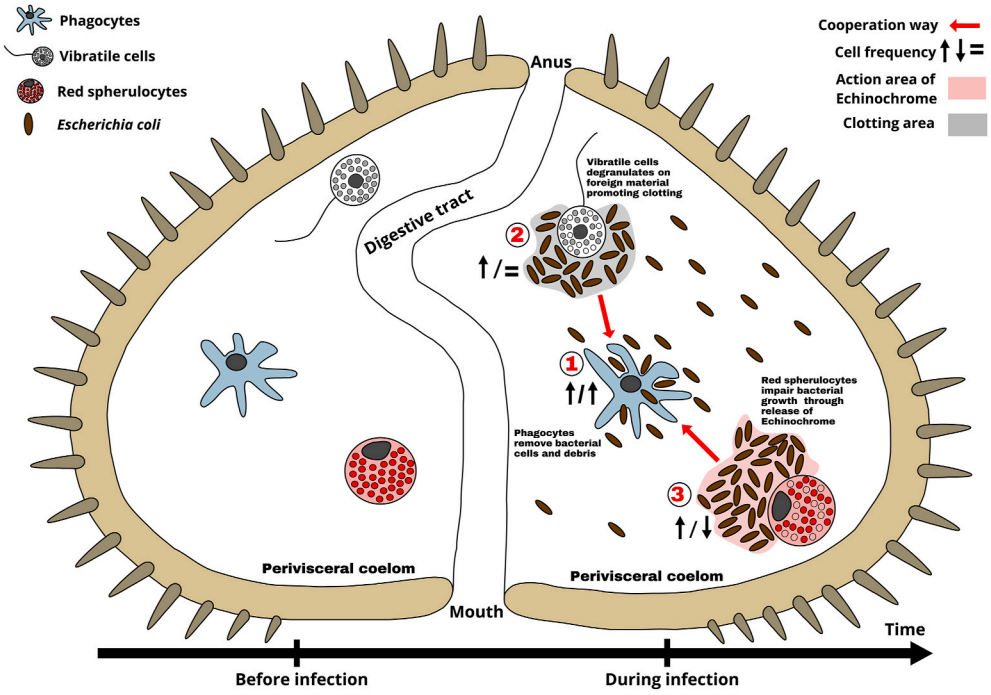

Fig. 5. Experimental immune challenge with *Escherichia coli* induces cell cooperation in the coelomocytes of *Arbacia lixula*. Schematic representation of the putative processes underlying the changes in coelomocytes frequency in *A. lixula*, based on the results obtained in this study. The presence of *E. coli* induces alterations in the frequencies of phagocytes (LE), vibratile cells (LC), and red spherulocytes (SC). The percentage of phagocytes (1), the coelomocytes responsible for removing foreign particles, increased (↑) during all period analyzed. On the other hand, the percentage of vibratile cells (2), which promote clotting, have a sharp decrease (↓) in the first 24 h and then remains stable (=). Red spherulocyte (3), a coelomocyte that presents antibacterial activity due to echinochrome, increase the percentage (↑) in the first 24 h and then decrease (↓) back to the control levels. After bacterial injection, phagocytes start to actively ingest bacterial cells, removing them from the coelomic fluid. Concomitantly, vibratile cells degranulate, trapping *E. coli* in a gelatinous clot and reducing its spreading in the coelomic cavity, while red spherulocytes release their bactericidal/bacteriostatic compound, the echinochrome. These two coelomocytes cooperate (red arrows) with the phagocytes, facilitating the removal of bacterial cells from the coelomic cavity.

immune response has been addressed (first 24 h), injection of LPS from *E. coli* was able to increase phagocytes and red spherulocytes percentages [9]. In the latter two, an initial decrease in cell counts was observed in the first 6 h after infection [21,48], followed by an increase after that [48].

Further important aspects can be seen in the intermediate region. In this gate, a noteworthy increase in cell frequency was observed in challenged individuals, compared to the control. We suggest two hypotheses to explain this sudden change: first, these changes may be a natural phenomenon in the coelomic fluid as coelomocytes can modify their shape, as previously observed in spherulocytes and phagocytes [22,45]; second, changes in proportions may be due to vibratile cells and red spherulocytes modifying their shapes by releasing their contents, along with the recruitment of circular and elongated cells during the inflammatory response. Given all results, the second hypothesis seems more plausible.

The variation in the abundance of vibratile cells, red spherulocytes, and large and small phagocytes in AL was certainly a physiological response to *E. coli* immune challenge. Red spherulocytes have a well-known antibacterial function [50], while phagocytes remove foreign particles, including bacteria [44]. In contrast, there is no experimental evidence on vibratile cell function. Some *in vitro* observations have pointed out that this cell population seems to be involved in defense mechanisms by degranulating during coagulation events ([6,51,52]. According to Johnsson [51], vibratile cells of *Strongylocentrotus* were able to 'cause temporary stasis of the coelomic fluid in areas of invasion by foreign liquid and other foreign material'. Smith et al. [45] stated that 'clotting could be an important physiological response, functioning to block the loss of coelomic fluid, and to sequester pathogens and prevent their invasion throughout the body'. Furthermore, a recent study showed that lipopolysaccharides can elicit cell aggregation [41]. Therefore, we hypothesized that vibratile cells and red spherulocytes may be cooperating with the phagocytes in the immune response of AL (Fig. 5). Based on our results, the reduction of LC and the increase, followed by a subsequent decrease, in SC cells (*i.e.* vibratile cells and red spherulocytes respectively) can be interpreted as a response to prevent the spreading and proliferation of bacteria. Vibratile cells could thus be involved in clotting reactions, possibly to immobilize pathogens [6,51,52] while red spherulocytes act antibiotically by releasing echinochrome-A [50]. Concomitantly, the increase in the number of phagocytes (elongated cells) to cleanse the coelomic fluid of pathogens or foreign particles is a fact already observed in other species [9,21]. This sequence explains why the number of red spherulocytes increases after 24 h, with a subsequent decrease; and vibratile cells decreased in the first 24 h and then remained stable, whereas the number of phagocytes increased consistently in the entire period (Fig. 5).

5. Conclusions

The technique used in the present study was suitable for both cell characterization and physiological investigation. Immediate coelomocyte fixation with 2.5% glutaraldehyde, a typical fixative for electron microscopy analyses, helped retain the flagellum of vibratile cells and prevented substantial changes in phagocyte shape (*cf.* Figs. 2 and 3), as previously reported [42]. However, the conspicuous morphology of red spherulocytes was not conserved. Instead, a small corpuscle was observed, which was considerably opaque due to the loss of pigments during fixation. This is supported by two observations: (i) most red spherulocytes observed using light microscopy (data not shown) presented the typical red coloration but appeared shrunken, and (ii) the fixative solution turned reddish during the process, indicating that the cellular content of red spherulocytes partially leaked into the solution. Regarding phagocytes, it is possible that the three different subpopulations, *i.e.* discoidal, polygonal, and small phagocyte, show only two morphologies while in suspension in the physiological coelomic fluid and can only be differentiated after spreading on a flat surface. Moreover, the use of PI provided more reliable information as intact cells were differentiated from debris, and the noise was thus removed

from the data.

Taken together, the use of IFC can provide fast and more accurate measurements to study the physiology of echinoderms, such as in studies on immune parameters and/or using coelomocytes as an endpoint [15, 38], or on aquaculture [53,54]. This method can provide new insights in coelomocyte studies and has previously been applied in other phyla [23, 24]. With the present study, we provide, for the first time, parameters for IFC that can be used for diverse approaches as well as the first experimental evidence about vibratile cell function. This is evidenced by our results on *A. lixula* coelomocyte subpopulation dynamics in response to experimental bacterial immune challenge. We suggest that different coelomocyte populations cooperate during infections. Vibratile cells and red spherulocytes may be involved in initial immobilization through clotting and antibiosis, respectively, whereas phagocytes are responsible for removing foreign particles from the coelomic cavity. However, further studies on vibratile cells are needed, as a reliable morphological characterization and analysis of the compounds it contains are lacking. Still, it is necessary to know how the early cellular response in the coelomic cavity happens, which will certainly help to understand the real function of vibratile cells during foreign invasions.

Declaration of competing interest

The authors declare that there are no conflicts of interest.

Acknowledgements

The authors thank Prof. Regina P. Markus, Prof. Pedro A. C. M. Fernandes, and the “Central de Aquisição de Imagens e Microscopia” (CAIMI) from the Instituto de Biociências of the Universidade de São Paulo for the use of the FlowSight Amnis (FAPESP 2014/20809-1). The authors are especially thankful to the anonymous referees, whose comments greatly improved the manuscript. Sandra M. Muxel and Vinicius Queiroz thanks FAPESP (Grant numbers: 2018/24693-9 (SMM), 2015/21460-5 and 2018/14497-8 (VQ)) for personal financial support. This is a contribution of NP-BioMar (Research Center for Marine Biodiversity - USP).

Appendix A. Supplementary data

Supplementary data to this article can be found online at https://doi.org/10.1016/j.fsi.2020.12.014.

Funding

This study was supported by the Fundação de Amparo a Pesquisa do Estado de São Paulo - FAPESP (Grant number: 2015/21460-5 and 2018/14497-8) and >Coordenação de Aperfeiçoamento de Pessoal de Nível Superior - Brazil (CAPES) Finance Code 001.

Credit author statement

The authors declare that they have no known competing financial interests or personal relationships that could have appeared to influence the work reported in this paper.

References

[1] D.L. Pawson, Phylum echinodermata, Zootaxa 1668 (2007) 749–764.
[2] F. Chia, J. Xing, Echinoderm coelomocytes, Zool. Stud. 35 (1995) 231–254.
[3] M. Vazzana, T. Siragusa, V. Arizza, G. Buscaino, M. Celi, Cellular responses and HSP70 expression during wound healing in *Holothuria tubulosa* (Gmelin, 1788), Fish Shellfish Immunol. 42 (2015) 306–315.
[4] M.T. Faria, J.R. da Silva, Innate immune response in the sea urchin *Echinometra lucunter* (Echinodermata), J. Invertebr. Pathol. 98 (2008) 58–62.
[5] C. Canicatti, G. D'Ancona, Cellular aspects of *Holothuria polii* immune response, J. Invertebr. Pathol. 53 (1989) 152–158.
[6] K. Bertheussen, R. Seljelid, Echinoid phagocytes in vitro, Exp. Cell Res. 111 (1978) 401–412.
[7] V. Queiroz, M.R. Custódio, Characterisation of the spherulocyte subpopulations in *Eucidaris tribuloides* (cidaroida: Echinoidea), Ital. J. Zool. 82 (2015) 338–348.
[8] V. Arizza, F. Giaramita, D. Parrinello, M. Cammarata, N. Parrinello, Cell cooperation in coelomocyte cytotoxic activity of *Paracentrotus lividus* coelomocytes, Comp. Biochem. Physiol. A: Mol. Integr. Physiol. 147 (2007) 389–394.
[9] M. Chiaramonte, L. Inguglia, M. Vazzana, A. Deidun, V. Arizza, Stress and immune response to bacterial LPS in the sea urchin *Paracentrous lividus* (Lamarck, 1816), Fish Shellfish Immunol. 92 (2019) 384–394.
[10] T. Haug, A.K. Kjuul, O.B. Styrvold, E. Sandsdalen, Ø.M. Olsen, K. Stensvåg, Antibacterial activity in *Strongylocentrotus droebachiensis* (Echinoidea), *Cucumaria frondosa* (holothuroidea), and *Asterias rubens* (asteroidea), J. Invertebr. Pathol. 81 (2002) 94–102.
[11] V. Matranga, A. Pinsino, M. Celi, A. Natoli, R. Bonaventura, H.C. Schröder, W.E. G. Müller, in: V. Matranga (Ed.), Monitoring Chemical and Physical Stress Using Sea Urchin Immune Cells, Echinodermata, Springer, Heidelberg, 2005, pp. 85–110.
[12] J. Lindsay, R.B. Lyons, R.L. Bacon, Separation of sea urchin coelomocyte types by centrifugation, Am. Zool. 15 (1965) 645.
[13] C.L. Smith, R.J. Britten, E.H. Davidson, SpCoel1: a seaurchin profilin gene expressed specifically in coelomocytes in response to injury, Mol. BioI. Cell 3 (1992) 403–414.
[14] L. I Messer, A.C. Wardlaw, Separation of the coelomocytes of *Echinus esculentus* by desnsity gradient centrifugation, in: A. A Balkema (Ed.), Proc. Eur. Col. Echin. Brussels, 1979, pp. 3–8.
[15] G. Coteur, M. Warnau, M. Jangoux, P. Dubois, Reactive oxygen species (ROS) production by amoebocytes of *Asterias rubens* (Echinodermata), Fish Shellfish Immunol. 12 (2002) 187–200.
[16] C. McCaughey, A. Bodnar, Investigating the sea urchin immune system: implications for disease resistance and aging, J. Young Investig. 23 (2012) 25–33.
[17] W. Lin, S. Grant, G. Beck, Generation of monoclonal antibodies to coelomocytes of the purple sea urchin *Arbacia punctulata*: characterization and phenotyping, Dev. Comp. Immunol. 31 (2007) 465–475.
[18] W.Y. Liao, S.D. Fugmann, Lectins identify distinct populations of coelomocytes in *Strongylocentrotus purpuratus*, PloS One 12 (2017), e0187987.
[19] J. Xing, H.S. Yang, M.Y. Chen, Morphological and ultrastructural characterization of the coelomocytes in *Apostichopus japonicus*, Aquat. Biol. 2 (2008) 85–92.
[20] A. Romero, B. Novoa, A. Figueras, Cell mediated immune response of the Mediterranean sea urchin *Paracentrotus lividus* after PAMPs stimulation, Dev. Comp. Immunol. 62 (2016) 29–38.
[21] M.A. Yui, C.J. Bayne, Echinoderm immunology: bacterial clearance by the sea urchin *Strongylocentrotur purpuratus*, Biol. Bull. 165 (1983) 473–486.
[22] L.C. Smith, V. Arizza, V. Hudgell, M.A.B. Barone, G. Bodnar, A.G. Buckley, R. Furukawa, Echinodermata: the complex immune system in echinoderms, in: E. Cooper (Ed.), Adv Comp. Immunol, Springer, Cham, 2018, pp. 409–501.
[23] R.T. Clark, Imaging flow cytometry enhances particle detection sensitivity for extracellular vesicle analysis, Nat. Methods 12 (2015) 1–2.
[24] J. Jiménez-Merino, I.S. de Abreu, L.S. Hiebert, S. Allodi, S. Tiozzo, C.M. De Barros, F.D. Brown, Putative stem cells in the hemolymph and in the intestinal submucosa of the solitary ascidian *Styela plicata*, EvoDevo 10 (2019) 1–19.
[25] B. Oliveira, P. Martinez, B. Simoes, C. Bispo, C. Andrade, C. Ferrario, R. Zilhao, A combined characterization of coelomic fluid cell types in the spiny starfish *Marthasterias glacialis*: inputs from flow cytometry and imaging, BioRxiv (2020), https://doi.org/10.1101/2020.06.20.163196.
[26] N.S. Barteneva, E. Fasler-Kan, I.A. Vorobjev, Imaging flow cytometry: coping with heterogeneity in biological systems, J. Histochem. Cytochem. 60 (2012) 723–733.
[27] M.V. Máximo, L.S.M. Mottola, C. Resgalla Jr., Sensibilidade do ouriço *Arbacia lixula* (Echinodermata: Echinoidea) em testes de toxicidade, J. Braz. Soc. Ecotoxicol. 3 (2008) 47–52.
[28] M.B. Alves, A.A. Emerenciano, I.C. Bordon, J.R.M.C.D. Silva, D.I. Fávaro, Biomonitoring evaluation of some toxic and trace elements in the sea urchin *Lytechinus variegatus* (Lamarck, 1816) in a marine environment: northern coast of Sao Paulo (Brazil), J. Radioanal. Nucl. Chem. 316 (2018) 781–790.
[29] I.A. Santos-Gouvea, C.A. Freire, Differences in ion regulation in the sea urchins *Lytechinus variegatus* and *Arbacia lixula* (Echinodermata: Echinoidea), J. Mar. Biol. Assoc. U. K. 87 (2007) 769.
[30] J.M. Sciani, A.K. Emerenciano, J.R.M.C.D. Silva, D.C. Pimenta, Initial peptidomic profiling of Brazilian sea urchins: *Arbacia lixula, Lytechinus variegatus* and *Echinometra lucunter*, J. Venom. Anim. Toxins Incl. Trop. Dis. 22 (2016) 17, https://doi.org/10.1186/s40409-016-0071-x.
[31] V. Queiroz, V. Arizza, M. Vazzana, H.E. Rozas, M.R. Custódio, Cytocentrifugation as an additional method to study echinoderm coelomocytes: a comparative approach combining living cells, stained preparations, and energy-dispersive x-ray spectroscopy, Rev. Biol. Trop. (2021). In press.
[32] P. Dunham, G. Weissman, Aggregation of marine sponge cells induced by Ca pulses, Ca ionophores, and phorbol esters proceeds in the absence of external Ca, Biochem. Biophys. Res. Commun. 134 (1986) 1319–1326, https://doi.org/10.1016/0006-291X(86)90394-3.
[33] V. Queiroz, Opportunity makes the thief—observation of a sublethal predation event on an injured sea urchin, Mar. Biodivers. 48 (2016) 153–154.
[34] J.F. Sambrook, D.W. Russel, V3, Molecular Cloning: A Laboratory Manual, third ed., Cold Spring Harbor Laboratory Press, 2001.
[35] Y.K. Lee, B.S. Soh, J.H. Wu, Quantitative assessment of phagocytic activity of hemocytes in the prawn, *Penaeus merguiensis*, by flow cytometric analysis, Cytometry A 43 (2001) 82–85.

[36] L. Canesi, C. Pruzzo, R. Tarsi, G. Gallo, Surface interactions between Escherichia coli and hemocytes of the Mediterranean mussel *Mytilus galloprovincialis* lam. leading to efficient bacterial clearance, Appl. Environ. Microbiol. 67 (2001) 464–468.
[37] E. Doussantousse, E. Pelletier, L. Beaulieu, L. Rainville, C. Belzile, Multixenobiotic resistance in coelomocytes from three echinoderm species, Aquat. Biol. 12 (2011) 81–96.
[38] L. Stabili, P. Pagliara, The sea urchin *Paracentrotus lividus* immunological response to chemical pollution exposure: the case of Lindane, Chemosphere 134 (2015) 60–66.
[39] J. Hira, D. Wolfson, A.J.C. Andersen, T. Haug, K. Stensvåg, Autofluorescence mediated red spherulocyte sorting provides insights into the source of spinochromes in sea urchins, Sci. Rep. 10 (2020) 1149, https://doi.org/10.1038/s41598-019-57387-7.
[40] P.S. Gross, L.A. Clow, L.C. Smith, SpC3, the complement homologue from the purple sea urchin, *Strongyloncentrotus purpuratus*, is expressed in two subpopulations of the phagocytic coelomocytes, Immunogenetics 51 (2000) 1034–1044.
[41] A.J. Majeske, C.J. Bayne, L.C. Smith, Aggregation of sea urchin phagocytes is augmented *in vitro* by lipopolysaccharide, PloS One 8 (2013), e61419. http://doi:10.1371/journal.pone.0061419.
[42] E.S. Kaneshiro, R.D. Karp, The ultrastructure of coelomocytes of the sea star *Dermasterias imbricata*, Biol. Bull. 159 (1980) 295–310.
[43] G. Coteur, G. DeBecker, M. Warnau, M. Jangoux, P. Dubois, Differentiation of immune cells challenged by bacteria in the common European starfish, *Asterias rubens* (Echinodermata), Eur. J. Cell Biol. 81 (2002) 413–418.
[44] L.C. Smith, J.P. Rast, V. Brockton, D.P. Terwilliger, S.V. Nair, K.M. Buckley, A. J. Majeske, The sea urchin immune system, Invertebr. Surviv. J. 3 (2006) 25–39.
[45] L.C. Smith, J. Ghosh, K.M. Buckley, L.A. Clow, N.M. Dheilly, T. Huag, J.H. Henson, C.L. ChengMan Lun, A.J. Majeske, V. Matranga, S.V. Nair, J.P. Rast, D.A. Raftos, M. Roth, S. Sacchi, C.S. Schrankel, K. Stensvag, Echinoderm immunity, in: K. Söderhäll (Ed.), Invertebrate Immunity, Landes Bioscience and Springer Science BusinessMedia, New York, 2010, pp. 260–301.
[46] F. Li, X. Chang, L. Xu, F. Yang, Different roles of crayfish hemocytes in the uptake of foreign particles, Fish Shellfish Immunol. 77 (2018) 112–119.
[47] D. Melillo, R. Marino, G. Della Camera, P. Italiani, D. Boraschi, Assessing immunological memory in the solitary ascidian *Ciona robusta*, Front. Immunol. 10 (2019) 1977, https://doi.org/10.3389/fimmu.2019.01977.
[48] B. Ptytycz, R. Seljelid, Bacterial clearance by the sea urchin *Strongylocentrotus droebrachiensis*, Dev. Comp. Immunol. 17 (1993) 283–289.
[49] F. Ramírez-Gómez, F. Aponte-Rivera, L. Méndez-Castaner, J.E. García-Arrarás, Changes in holothurian coelomocyte populations following immune stimulation with different molecular patterns, Fish Shellfish Immunol. 29 (2010) 175–185.
[50] C.J. Coates, C. McCulloch, J. Betts, T. Whalley, Echinochrome A release by red spherule cells is an iron-withholding strategy of sea urchin innate immunity, J. Innate Immunity. 10 (2018) 119–130.
[51] P.T. Johnson, The coelomic elements of sea urchins (*Strongylocentrotus*). I. The normal coelomocytes; their morphology and dynamics in hanging drops, J. Invertebr. Pathol. 13 (1969) 25–41.
[52] P.T. Johnson, The coelomic elements of the sea urchins (*Strongylocentratus*) III. In vitro reaction to bacteria, J. Invertebr. Pathol. 13 (1969) 42–62.
[53] R. Shannon, E. Blumenthal, A. Mustafa, Physiological and immunological responses in Giant California sea cucumbers (*Parastichopus californicus*) exposed to aquaculture-related stress, Bioengin. Biosci. 3 (2015) 60–67.
[54] R. Shannon, A. Mustafa, A comparison of stress susceptibility of sea urchins and sea cucumbers in aquaculture conditions, Bioengin. Biosci. 3 (2015) 100–107.